Scaling in Cohesive Self-gravitating Aggregates

Paul Sánchez, Emilien Azéma, Daniel J. Scheeres

Scaling in Cohesive Self-gravitating Aggregates Paul Sánchez[1], Emilen Azéma[2] and Daniel J. Scheeres[1], [1]Colorado Center for Astrodynamics Research, University of Colorado, Boulder, CO 80309-431, [2]*LMGC*, Université de Montpellier, CNRS, Montpellier, France (diego.sanchez-lana@colorado.edu).

By means of extensive three-dimensional contact dynamics simulations, we analyse the strength properties and microstructure of a granular asteroid, modelled as a self-gravitating cohesive granular aggregate composed of spherical particles, and subjected to diametrical compression tests. We show that, for a broad range of system parameters (shear rate, cohesive forces, asteroid diameter), the behaviour can be described by a modified inertial number that incorporates interparticle cohesion and gravitational forces.

Contact Dynamic Method: We will use the Contact Dynamic Method [1, 2, 3], that is a type DEM, originally developed by J.-J. Moreau in Montpellier, in which particles are assumed to be perfectly rigid and to interact through mutual exclusion and Coulomb friction. The frictional contact interactions are described as *complementarity relations* between the relative velocities between particles and the corresponding momenta at the contact points. The condition of geometrical contact between two particles is expressed by the following mutually exclusive alternatives, known as "Signorini's conditions":

$$\begin{array}{lll} f_n \geq 0 & \text{and} & u_n = 0, \\ f_n = 0 & \text{and} & u_n > 0. \end{array} \qquad (1)$$

where f_n is the normal contact force and u_n the relative normal velocity. u_n is counted positive when the particles move away from each other. In the same way, the Coulomb friction law involves the following three mutually exclusive conditions:

$$\begin{array}{rll} f_t = -\mu f_n & \text{and} & u_t > 0, \\ -\mu f_n \leq f_t \leq \mu f_n & \text{and} & u_t = 0, \\ f_t = \mu f_n & \text{and} & u_t < 0, \end{array} \qquad (2)$$

where u_t is the sliding velocity at the contact, μ is the friction coefficient and f_t is the friction force. Notice that none of the relations 1 and 2 can be reduced to a (mono)valued functional dependence between the two variables as assumed in the more common Soft-Sphere DEM (SSDEM). Hence, the only material parameter required within the CD-method is the particle-particle coefficient of friction μ, whereas in SSDEM packings are also characterised by normal and tangential stiffnesses as well as viscous damping parameters.

Procedure: First, we build a large sample of 10000 spherical particles under isotropic compression inside a box. The particles have a diameter $d \in [0.6d_{max}, d_{max}]$, with a uniform distribution per volume fraction. Friction, cohesion and gravitational forces are not yet activated. Density ρ_0 of the particles is fixed to $3200kg/m^3$. We extract spherical agglomerates of diameter D from this sample comprising nearly $N_p = 5000$ particles. In order to analyse the effect of aggregate size, four aggregates were built, with $d_{max} \in [3, 6, 12, 18]$m, so D is approximately $[50, 100, 190, 375]$m. Then, the friction coefficient is fixed to 0.4, cohesive forces, modelled as a constant reversible attractive force $-f_0$ with a short range action of the order of $0.01d$, are activated. Gravitational forces are represented by $F_{g_0} = \pi d^3 \rho_0 g_0 r/(6D)$ acting on the centre of each particle at a distance r of the centre of the aggregate and pointing towards it. The aggregates are then subjected to diametrical compression between two platens, with a prescribed velocity $V_{wall} = \dot{\gamma} D$ (see Fig. 1(a)). I_η and η were varied between $[5.10^{-4}, 0.1]$ and $[0.1Pa, .., 100MPa]$, respectively. We performed simulations for a broad range of combinations of these two parameters for both, non-gravitational and gravitational aggregates. When gravitational forces are included, P_0 increases with D, from ~ 0.48Pa, to ~ 30Pa.

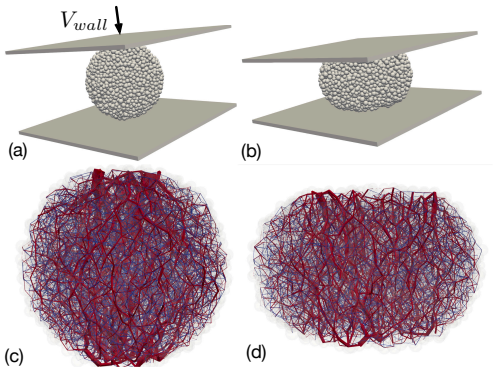

Figure 1: Snapshots of a simulated granular asteroid under diametrical compression for $\varepsilon_h = 0$ (a) and $\varepsilon_h = 0.1$(b). Forces chains are represented by lines joining the centres of two touching particles. Compressive forces in red, tensile forces in blue.

During diametrical compression, the vertical stress σ_{zz} acting on an aggregate is given by $4F/\pi D^2$, where F is measured on the platen.

Figure 2 shows σ_{zz} as a function of the axial deformation ε_h for $\eta = 1Pa$, $D = 50m$ and different values of I_η, and for $I_\eta = 5 \times 10^{-4}$ with different values of η (inset). ε_h is the classical cumulative vertical deformation defined by $\Delta D/D$ with $\Delta D = D - D_t$ with D_t the height of the wall at the time t. As a general observation, at small I_η values, the stress-strain curve is well defined and has very small deviations around the mean. The stress increases to a peak value at small

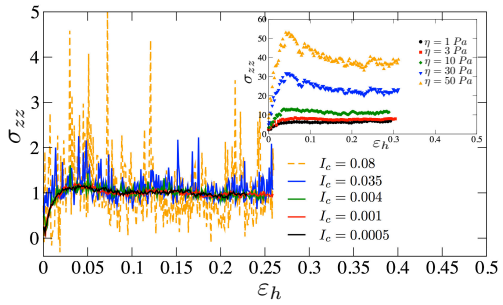

Figure 2: Typical curve showing the vertical strength as a function of the cumulative vertical deformation for $\eta = 1Pa$, $D = 50m$ and various values of I_η (gravitational forces are not activated). The inset shows the same curve for $I_c = 5.10^{-5}$, $\eta = \{1, 3, 10, 30, 50\}Pa$ for $D = 190m$ considering gravitational forces.

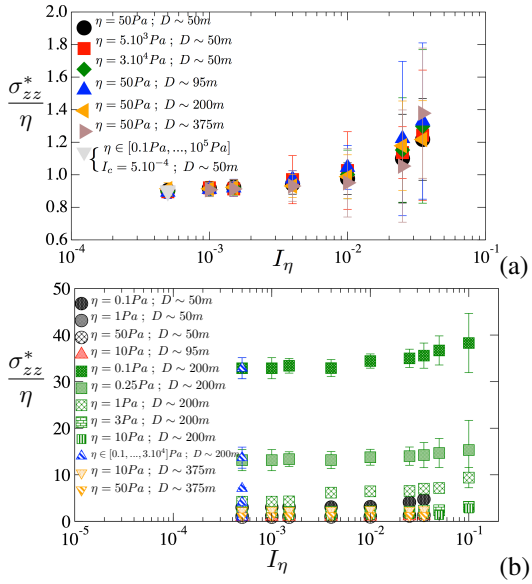

Figure 3: Peak stress σ^*_{zz} normalized by the cohesive stress η as a function of I_η (a) without gravitational forces (i.e. $I_{g_0} = 0$), and (b) with gravitational forces (i.e. $I_{g_0} \neq 0$), in which only one or two parameters were varied.

strain ($\approx 2\%$) before relaxing to a constant plateau (plastic behaviour) at larger strain. Deformations are localised in the vertical plane of the aggregate, where compressive force chains are mainly vertical and tensile force chains lie horizontally (see Fig. 1(b)). This ductile behaviour results from particle rearrangements, dissipation due to friction and the short-range action of cohesive forces. As I_η increases, fluctuations in the stress-strain responses increase both in number and magnitude revealing a dynamical crisis. Thus, in the following we consider only results for $I_\eta < 0.035$ for non-gravitational aggregates and $I_\eta < 0.1$ for gravitational ones; the peak stress σ^*_{zz} is defined as an average stress around a deformation of 2%.

In the absence of gravitational forces, we naturally

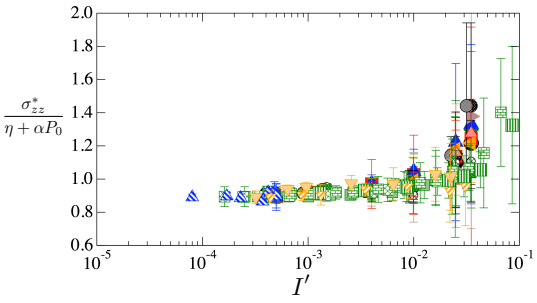

Figure 4: Peak stress σ^*_{zz} normalised by additive stress $p = \eta + \alpha P_0$ as a function of the modified inertial number I' for the raw data (color coding as in Fig 3). Error bars represent the standard deviation around the peak state.

expect σ^*_{zz} to scale with η since cohesion is homogeneously distributed in all contacts. This is well observed in Fig. 3(a) for a wide range of values of I_η, η and D. In contrast, when gravitational forces are active, the scaling with η is not verified (see Fig. 3(b)). This is because the effect of gravity is to increase the local stresses acting on the particles, so that interparticle tensile strength and interior stresses become additive. We can thus postulate that the mean pressure is $p = \eta + \alpha P_0$, where α is a weight parameter that represents the stress gradient produced by the radial variation of the gravitational field inside an aggregate. A similar approach has been used for the scaling of shear stresses in dense suspensions [4, 5] and in cohesive granular flow [6], where the fluid or cohesive forces and grain stresses are responsible for the effective friction angle. Accordingly, the inertial number can be re-written as:

$$I' = \dot{\gamma} d \sqrt{\frac{\rho_0}{\eta + \alpha P_0}} = \frac{I_\eta}{\sqrt{1 + \alpha \lambda^{-1}}} = \frac{I_\eta . I_{g_0}}{\sqrt{I^2_{g_0} + \alpha I^2_\eta}} \quad (3)$$

Figure 4 shows σ^*_{zz} normalised by $(\eta + \alpha P_0)$ as a function of I', for $\alpha = 0.48$. We observe the collapse of all our simulation data with a pre-factor $\simeq 0.9$ for small I' values. This pre-factor (and fluctuations around the mean) increases with I' to 1.3 in the range of values tested here, evidencing the dynamical crisis resulting from the destabilising effect of particle inertia.

References: [1] J. J. Moreau (1994) *Eur J Mech A* 13:93. [2] J.-J. Moreau (2004) in *Novel approaches in civil engineering* (Edited by M. Fremont, et al.) 1–46 Springer-Verlag ISBN 978-3-540-45287-4. [3] M. Jean (1999) *Computer Methods in Applied Mechanics and Engineering* 177:235. [4] M. Trulsson, et al. (2012) *Physical Review Letters* 118305(SEPTEMBER):1 doi. [5] L. Amarsid, et al. (2017) 012901 doi. [6] N. Berger, et al. (2015) *European physical Letters* 112(64004).